HHS Public Access

Author manuscript

Redox Biochem Chem. Author manuscript; available in PMC 2024 December 26.

Published in final edited form as:

Redox Biochem Chem. 2024 December ; 10: . doi:10.1016/j.rbc.2024.100043.

Dysfunctional copper homeostasis in *Caenorhabditis elegans* affects genomic and neuronal stability

Ann-Kathrin Weishaupt[a,b], **Anna Gremme**[a], **Torben Meiners**[a], **Vera Schwantes**[c], **Karsten Sarnow**[a], **Alicia Thiel**[a], **Tanja Schwerdtle**[b,d], **Michael Aschner**[e], **Heiko Hayen**[c], **Julia Bornhorst**[a,b,*]

[a]Food Chemistry with Focus on Toxicology, Faculty of Mathematics and Natural Sciences, University of Wuppertal, Germany

[b]TraceAge – DFG Research Unit on Interactions of Essential Trace Elements in Healthy and Diseased Elderly (FOR 2558), Berlin-Potsdam-Jena-Wuppertal, Germany

[c]Institute of Inorganic and Analytical Chemistry, University of Münster, Germany

[d]German Federal Institute for Risk Assessment (BfR), Berlin, Germany

[e]Department of Molecular Pharmacology, Albert Einstein College of Medicine, Bronx, NY, USA

Abstract

While copper (Cu) is an essential trace element for biological systems due to its redox properties, excess levels may lead to adverse effects partly due to overproduction of reactive species. Thus, a tightly regulated Cu homeostasis is crucial for health. Cu dyshomeostasis and elevated labile Cu levels are associated with oxidative stress and neurodegenerative disorders, but the underlying mechanisms have yet to be fully characterized. Here, we used *Caenorhabditis elegans* loss-of-function mutants of the Cu chaperone ortholog atox-1 and the Cu binding protein ortholog ceruloplasmin to model Cu dyshomeostasis, as they display a shifted ratio of total Cu towards labile Cu. We applied highly selective and sensitive techniques to quantify metabolites associated to oxidative stress with focus on mitochondrial integrity, oxidative DNA damage and neurodegeneration all in the context of a disrupted Cu homeostasis. Our novel data reveal elevated oxidative stress, compromised mitochondria displaying reduced ATP levels and cardiolipin content. Cu dyshomeostasis further induced oxidative DNA damage and impaired DNA damage

*Corresponding author. Gaußstraße 20, 42119, Wuppertal, Germany. bornhorst@uni-wuppertal.de (J. Bornhorst).

Declaration of competing interest

The authors declare that they have no known competing financial interests or personal relationships that could have appeared to influence the work reported in this paper.

CRediT authorship contribution statement

Ann-Kathrin Weishaupt: Writing – original draft, Visualization, Methodology, Investigation, Conceptualization. **Anna Gremme:** Writing – review & editing, Methodology, Investigation. **Torben Meiners:** Writing – review & editing, Investigation. **Vera Schwantes:** Writing – review & editing, Methodology, Investigation. **Karsten Sarnow:** Writing – review & editing, Investigation. **Alicia Thiel:** Writing – review & editing, Methodology. **Tanja Schwerdtle:** Writing – review & editing. **Michael Aschner:** Writing – review & editing. **Heiko Hayen:** Writing – review & editing, Supervision. **Julia Bornhorst:** Writing – review & editing, Supervision, Funding acquisition, Conceptualization.

Appendix A. Supplementary data

Supplementary data to this article can be found online at https://doi.org/10.1016/j.rbc.2024.100043.

response as well as neurodegeneration characterized by behavior and neurotransmitter analysis. Our study underscores the essentiality of a tightly regulated Cu homeostasis as well as mitochondrial integrity for both genomic and neuronal stability.

Keywords

Copper dyshomeostasis; Oxidative stress; Mitochondrial impairment; Cardiolipins; Genomic and neuronal instability

1. Introduction

Copper (Cu) is an essential trace element and micronutrient, participating in many physiological pathways as an enzyme cofactor [1]. Due to the overuse of Cu-containing chemicals and fungicides in industry and agriculture, Cu is increasingly introduced into the environment, leading to a global concern [2]. When exceeding the physiological range, Cu leads to the formation of reactive oxygen and nitrogen species (RONS) due to its redox activity, which may affect macromolecules such as lipids or the DNA [3]. Therefore, a tightly regulated Cu homeostasis is crucial, since a Cu imbalance has been reported to induce oxidative stress as well as neurodegeneration [4,5]. In a previous study, we demonstrated that a dysregulated Cu homeostasis results in elevated labile Cu levels in *Caenorhabditis elegans* (*C. elegans*) [6]. Besides total Cu levels and the activity of the Cu storage protein ceruloplasmin, labile Cu is discussed to be an additional marker for Cu status, as it is readily available for cellular uptake [7]. As previously shown, a Cu imbalance leads to a shift from bound Cu towards pools of labile Cu [6], which is associated with the loss of antioxidant defense, impaired energy production and in turn mitochondrial deficits [4]. Indeed, Alzheimer's disease (AD) has been posited to result from Cu imbalance based on a correlation between brain Cu levels and the prevalence of AD [8]. The underlying mechanisms remain unknown, but are often linked to oxidative stress, which is induced by an imbalance of RONS and antioxidants [9]. Cells are equipped with a variety of enzymes and small molecules for antioxidative defenses [10]. Reduced and oxidized glutathione are key markers for oxidative stress [9,10]. As previously stated, RONS can damage macromolecules, such as lipids. Malondialdehyde (MDA), a degradation product of lipid peroxidation of polyunsaturated fatty acids is a common biomarker of oxidative stress [11]. A unique type of phospholipid class, exclusively present in mitochondria, are cardiolipins (CL) [12]. CLs have recently emerged in the focus of neurodegenerative diseases, as a reduction in CL levels has been linked to oxidative stress and mitochondrial dysfunction in AD [13]. Wilson's disease (WD), a Cu metabolism disorder resulting in neurological deficits, is characterized by a mutation in the *Atp7b* gene. This results in non-expression of the Cu exporter protein Atp7b, thereby leading to Cu accumulation, primarily in the liver, but also in the brain [5]. Studies reveal a progressive degradation of CLs in liver mitochondria of a WD mouse model ($Atp7b^{-/-}$) [14], which underlines the link between CLs and the pathogenesis of neurodegenerative diseases [12]. Massive RONS formation induced by Cu may further increase DNA lesions. An induction of DNA damage in response to elevated brain Cu levels was observed in AD, Parkinson's disease (PD), as well as in WD

[15]. However, the mode of action of Cu-induced toxicity and neurotoxicity is still under debate.

This study aims to investigate the molecular mechanisms of labile Cu redox biology using the model organism *C. elegans*. The nematode is a well-established model to examine metal-induced oxidative stress and neurotoxicity [16]. In addition, *C. elegans* conserved similar proteins related to the mammalian Cu metabolism, making it suitable for its investigation. Furthermore, we recently demonstrated that the nematode can model Cu homeostasis. Our previous study revealed that deletion mutants lacking cuc-1 (ortholog in humans is atox-1) and F21D5.3 (ortholog in humans are ceruloplasmin and hephaestin [17]) take up less total Cu, but display elevated levels of labile Cu compared to wildtype worms [6]. Our former study underlines the functionality of atox-1 and ceruloplasmin in the Cu homeostasis in *C. elegans*. Our aim is to elucidate the toxic mechanisms upon a disrupted Cu homeostasis regarding oxidative stress, with special focus on mitochondrial integrity in terms of energy-related nucleotides such as ATP, as well as total CL levels and the CL profile. Furthermore, the consequences of oxidative stress on genomic and neuronal stability due to Cu dyshomeostasis in *C. elegans* will be investigated.

2. Material and methods

2.1. C. elegans handling and treatment

C. elegans strain Bristol N2 (wildtype) and TJ356 (daf-16::GFP) were obtained from the Caenorhabditis Genetics Center (CGC, Minneapolis, USA), which is funded by the National Institutes of Health Office of Research Infrastructure Programs. Additionally, deletion mutants (Δ) of *cuc-1* (tm1220 (atox-1Δ)) and *f21d5.3* (tm14205 (ceruloplasminΔ)) were obtained from the Mitani Lab at Tokyo Women's Medical University. The worms' genotype was verified by single worm PCR using the following primers: *atox-1* forward: CAACTCGAATGGTTTAAGCAAC, reverse: GCTAGCATCAGATAATACGAC. *F21d5.3* forward: GCCTGGAGCACCAGTTGTAG, reverse: TGAAGCCACTGACCTCCATC. All strains were cultivated on 8P and NGM agar plates, which have been coated with *Escherichia coli* (*E. coli*) and maintained at 20 °C as previously described [18]. All experiments were performed using synchronous worms [19], which were placed on NGM agar plates until L4 larval stage. L4 stage worms were treated with Cu-enriched inactivated *E. coli* ($CuSO_4$ ≥99.99 %, Sigma Aldrich) on NGM plates for 24 h up to 2 mM for every experiment as previously shown [6]. Optionally, 100 mM paraquat (PQ)-enriched *E. coli* for 24 h (Sigma Aldrich) or 6.5 mM *tert*-butyl hydroperoxide (*t*-BOOH) (Sigma Aldrich) for 1 h in 85 mM NaCl solution were used as positive controls, but in wildtype worms only to verify assay procedures.

2.2. Daf-16 translocalization in daf-16::GFP mutants

Worm strain daf-16::GFP was used to assess daf-16 translocalization by fluorescence microscopy. After Cu treatment, worms were transferred to 4 % agarose pads on microscope slides and anesthetized using 5 mM levamisole (Sigma-Aldrich). Analysis was performed using DM6 B fluorescence microscope and the Leica LAS X software (Leica Microsystem GmbH). GFP localization was assessed and categorized as 1) present in cytosol, 2) as

intermediate or 3) localized into nucleus. For each experiment, ~25 worms were analyzed for each condition.

2.3. Gene expression via quantitative real-time PCR analysis

For gene expression assessment, RNA was isolated in pellets containing 500 worms as previously published using the Trizol method [20], which was transcribed using the High Capacity cDNA Reverse Transcription Kit (Applied Biosystems, Thermo Fisher Scientific) as stated in the manufacturer's protocol. Quantitative real-time PCR was carried out using TaqMan Gene Expression Assay probes (Applied Biosystems, Thermo Fisher Scientific) on an AriaMx Real-Time PCR System (Agilent). For normalization by the comparative $2^{-\Delta\Delta Ct}$ method, we used *AFDN* homolog *afd-1* as housekeeping gene [21]. The following probes were used: *afd-1* (Ce0241573_m1), *sod-1* (Ce02434432_g1), *sod-4* (Ce02451138_g1), *skn-1* (Ce02434432_g1), *bli-3* (Ce02413442_m1), *mpk-1* (Ce02445290_m1), *pmk-1* (Ce02456381_g1), *nsy-1* (Ce02432208_g1), *daf-16* (Ce02422838_m1), *gcs-1* (Ce02436726_g1), *pme-1* (Ce02415136_m1) and *pme-2* (Ce02437339_g1).

2.4. Glutathione (GSH and GSSG) levels quantification by HPLC-MS/MS

Reduced (GSH) and oxidized (GSSG) glutathione levels were assessed by liquid-chromatography tandem-mass spectrometry (HPLC-MS/MS). Following Cu treatment, pellets were prepared by centrifugation of 1000 worms in 100 µL 85 mM NaCl. Sample preparation and GSH/GSSG analysis was performed as previously published [22].

2.5. HPLC-DAD analysis of energy-related adenine and pyridine nucleotides

Sample preparation as well as analysis by ion-pair reversed phase HPLC were performed according Bornhorst et al. [23]. 2000 worms were pelletized per condition in 100 µL 85 mM NaCl and immediately prepared as stated. The analysis was performed on an Agilent 1260 Infinity II liquid chromatography system with a photodiode array detector (DAD). Nucleotide contents were evaluated by external calibration of standard solutions of adenosine triphosphate (ATP), adenosine diphosphate (ADP), adenosine monophosphate (AMP), nicotinamide adenine dinucleotide phosphate (NADPH) and nicotinamide adenine dinucleotide (NADH and NAD^+). Detection by DAD was performed at 259 nm and data analysis was carried out using the OpenLab (version 3.6) software (Agilent).

2.6. Quantification of malondialdehyde

Unbound and bound MDA were determined by high performance liquid chromatography with fluorescence detection (HPLC-FLD). The sample preparation was based on Grintzalis et al. [24] and optimized for *C. elegans* matrix. Phosphate buffer (3.54 g/L KH_2PO_4, 7.24 g/L Na_2HPO_4, pH 7.0) was stored at 4 °C. Following pelletizing of 2000 worms in 100 µL 85 mM NaCl, 200 µL phosphate buffer and 1.5 µL 0.1 M 2-and-3-*tert*-butyl-4-hydroxyanisol (BHA) (Sigma Aldrich) were added and the pellet was stored at −80 °C up to one week. Samples were homogenized by 3 × freeze-thaw cycles (1 min liquid nitrogen, 1 min 37 °C), 3 × sonication with an ultrasonic probe (20 s, cycle 1, amplitude 100 %; UP100H, Hielscher) and in an ultrasonic bath (5 min). After centrifugation (5 min, 18 620 rcf, 4 °C),

30 μL were transferred for protein measurement. 63 μL of 100 % trichloroacetic acid (TCA) (Carl Roth) were added, following 5 min incubation on ice. Samples were centrifuged (15 min, 20 000 rcf, 4 °C) and the entire supernatant (unbound MDA fraction) was transferred to a new tube and stored on ice until further use. For alkaline hydrolysis, 250 μL 1 M NaOH were added to the remaining pellet and incubated for 30 min at 60 °C. The hydrolyzed samples (bound MDA fraction) were cooled on ice and 25 μL conc. HCl was added. 1,1,3,3-Tetramethoxypropane (TMP) (Sigma Aldrich) was used for external calibration (20–500 nM), which forms an MDA-TBA product by derivatization with 2-Thiobarbituric acid (TBA) (Sigma Aldrich). For derivatization, 12.5 g/L TBA solution was prepared just before use by mixing solution A (100 % TCA, conc. HCl, ratio 5:1) and solution B (25 g/L TBA in 0.2 M NaOH) in a ratio of 1:1.50 μL 12.5 g/L TBA and 3 μL 0.1 M BHA were added to 200 μL of each a) unbound, b) bound MDA sample and c) TMP calibration solution. All solutions were heated at 100 °C for 20 min and 300 μL butanol was added after cooling. Following centrifugation (5 min, 20 000 rcf, 4 °C), MDA levels were analyzed in an aliquot of the 1-butanol phase. Settings for the HPLC-FLD analysis as well as method validation parameters are listed in the Supplementary.

2.7. Cardiolipin levels and distribution by 2D-LC-HRMS

Cardiolipins were analyzed by 2D-HPLC-HRMS analysis. A detailed overview of the sample preparation and instrument parameters is listed in the Supplementary.

2.8. 8oxodG measurement via ELISA

8-oxoguanine (8oxodG) has been quantified by the OxiSelect™ Oxidative DNA Damage ELISA kit (Cell Biolabs). 2000 worms were treated with Cu and pelletized as stated above. In the first step, DNA was isolated of each sample using the Qiagen Tissue and Blood DNA extraction kit, following the manufacturer's instruction. The amount of DNA was quantified by NanoDrop measurements and portioned in 40 μg aliquots, which were dried. In the second step, DNA was hydrolyzed by enzymes to obtain mononucleotides as described by Nicolai et al. [25]. As third step, 8-oxodG measurement was performed according the above-mentioned manufacturer's kit instructions.

2.9. HPLC-MS/MS analysis of PARylation levels

Sample preparation for poly-(ADP-ribose) (PAR) extraction was done in pellets of 1000 worms and according [25]. Analysis was performed by HPLC-MS/MS using an Agilent 1290 Infinity II liquid chromatography system (Agilent, Waldbronn, Germany), which is coupled to a Sciex QTRAP 6500+ triple quadrupole mass spectrometer (Sciex, Darmstadt, Germany). PAR quantification was assessed as described in Ref. [25], with minor changes in chromatography: Chromatographic separation was performed using a Hypersil Gold aQ 150 × 2.1 mm and corresponding 10 × 2.1 mm pre-column. Elution was carried out with bidistilled water +0.1 % formic acid (FA) and acetonitrile + 0.1 % FA and a flow of 0.3 mL/min. Total run time was 5 min, starting with 0–25 % of ACN in 2.5 min, to 100 % ACN in 0.5 min, 100 % ACN for 1 min, following re-equilibration to 0 % ACN. Results were normalized to DNA content determined by Hoechst method [26].

2.10. Neurotransmitter quantification via HPLC-MS/MS

Dopamine, serotonin, γ-amino butyric acid and acetylcholine levels were determined by HPLC-MS/MS. Pellets of 1000 worms per 50 μL 85 mM NaCl were prepared after Cu incubation. Samples were added with 100 μL extraction buffer, processed and analyzed according to Ref. [16]. Results were normalized to protein content analyzed by BCA assay (Sigma-Aldrich).

2.11. Aldicarb-induced paralysis assay

The assay is based on Mahoney et al. [27] and was performed as previously published [16]. Plates with 2 mM aldicarb (stock solution in 70 % EtOH) were always prepared fresh and the assay was performed as a blinded experiment at all times.

2.12. Statistical analysis

Statistical analysis was carried out using GraphPad Prism 6 (GraphPad Software, La Jolla, USA) using 2-way ANOVA with Tukey's multiple comparison or impaired *t*-test for one-to-one comparison. Significance level with $\alpha = 0.05$: *: $p \leq 0.05$; **: $p \leq 0.01$ and ***: $p \leq 0.001$ compared to untreated control and §: $p \leq 0.05$; §§: $p \leq 0.01$ and §§§: $p \leq 0.001$ compared to wildtype in same condition.

3. Results

3.1. Daf-16 translocation visualized by daf-16::GFP fluorescence microscopy and mRNA levels of mitogen-activated protein kinases

Protein kinases activated by stress, such as c-Jun N-terminal kinases (JNK) and p38 mitogen-activated kinases (MAPK), can stimulate Forkhead box O-class proteins (FoxO) expression and translocation from cytosol to nucleus, where it acts as transcription factor participating in DNA repair, RONS detoxification and apoptosis (Fig. 1A) [28]. The homolog of human FOXO3 is daf-16 in *C. elegans*, which can be visualized in the transgenic strain daf-16::GFP by fluorescence microscopy (Fig. 1B). 24 h treatment with $CuSO_4$ or PQ used as positive control leads to a significant translocation of daf-16 from cytosol into the nucleus (Fig. 1C). Furthermore, we examined mRNA levels of *daf-16/FOXO3* itself, but also representatives of MAPK's subgroups p38, JNK and ERK1/2 (extracellular signal-regulated kinases): *pmk-1/MAPK11*, *nsy-1/MAP3K5* and *mpk-1/MAPK1*. Gene expression of *daf-16/FOXO3* as well as of the p38 and JNK kinases *pmk-1/MAPK11* and *nsy-1/MAP3K5* are not altered due to Cu treatment (Supplementary), while ERK1/2 MAP kinase *mpk1/MAPK1* is upregulated in wildtype worms in a dose-dependent manner (Fig. 1D). Cu does not elevate mRNA levels of *mpk-1/MAPK1* in atox-1 and ceruloplasmin-deficient worms, but basal levels are already increased to the level of Cu-treated wildtype worms.

3.2. Reduced and oxidized glutathione, gcs-1/GCLC mRNA levels and energy-related nucleotides

As a marker for the antioxidative capacity, reduced (GSH) and oxidized (GSSG) glutathione were quantified by HPLC-MS/MS. Cu exposure (2 mM) significantly reduced GSH levels by 23 % in wildtype worms, 34 % in atox-1 and 38 % in ceruloplasmin deletion mutants

(Fig. 2A). Inversely, Cu elevates oxidized GSSG levels in all strains (Fig. 2B), however, ceruloplasmin-deficient worms display significantly lower GSSG levels after 2 mM Cu treatment compared to wildtype worms. *Gcs*-1/GCLC, which is involved in GSH synthesis, is not altered upon Cu incubation in *C. elegans*, but mutants with impaired Cu homeostasis display elevated mRNA levels (Fig. 2C). Energy-related nucleotides of interest, namely ATP, ADP, AMP, NADPH, NADH and NAD^+ were assessed by HPLC-DAD analysis (Fig. 2D–I). For all analytes tested, no alterations were detected by Cu treatment in wildtype worms. On the other hand, altered nucleotide levels were observed for the mutants displaying Cu dyshomeostasis, with ceruloplasmin-deficient worms seem to be specifically affected. Ceruloplasmin deletion mutants displayed reduced ATP levels compared to wildtype worms, which are further reduced following Cu incubation. Furthermore, ADP and AMP levels were increased by Cu in atox-1 as well as ceruloplasmin mutants. While NADPH levels were elevated in atox-1-deficient worms, they were significantly reduced in ceruloplasmin-deficient worms. Moreover, both mutants contained lesser NADH levels compared to wildtype worms, and this effect was more pronounced in ceruloplasmin-deficient worms and was further exacerbated by Cu treatment. In addition, ceruloplasmin-deficient worms showed increased NAD^+ levels following Cu treatment.

3.3. Malondialdehyde quantification and total cardiolipin levels and distribution

Using alkaline hydrolysis, unbound MDA as well as bound MDA, for example bound to proteins or DNA, were assessed. Our data reveal no alterations induced by Cu or *t*-BOOH on the amount of bound MDA (Supplementary). However, unbound MDA levels increased significantly by *t*-BOOH in wildtype worms as well as by Cu treatment in the deletion mutants atox-1 and ceruloplasmin (Fig. 3A). CLs are exclusively found in mitochondria and are fundamental for the mitochondrial membrane [13]. Our data showed no significant alterations in the CL profile induced by Cu supplementation in the tested worm strains but of the total CL content in the deletion mutant ceruloplasmin was reduced compared to wildtype worms (Fig. 3B). Furthermore, our data revealed no alterations induced either by Cu supplementation or genetic Cu dyshomeostasis on the relative distribution of CL species with respect to chain length and the degree of saturation (Fig. 3C and Supplementary).

3.4. Oxidative DNA damage (8oxodG), DNA damage response (PARylation) and pme/PARP mRNA levels

We assessed levels of 8-oxoguanine (8oxodG), which is the most common DNA lesion initialized by RONS [29], as well as poly-(ADP-ribosylation) (PARylation) as a marker for DNA damage response. Data reveal increased 8oxodG levels for ceruloplasmin-deficient worms up to 350 % following 2 mM Cu treatment, while wildtype and atox-1-deficient worms remained unaffected (Fig. 4A). PAR levels showed no alterations in wildtype and ceruloplasmin mutants due to Cu supplementation. In contrast, untreated atox-1 mutants displayed reduced PAR levels compared to wildtype worms, but increased PARylation following Cu treatment (Fig. 4B). Furthermore, mRNA levels of NAD^+-dependent poly (ADP-ribose) polymerases (PARP), were examined (Fig. 4C + D). While *pme-1/PARP1* remained unchanged, *pme-2/PARP2* was downregulated to about 50 % in untreated atox-1-deficient mutants compared to wildtype worms, yet it was upregulated in response to Cu treatment.

3.5. Quantification of neurotransmitters DA, SRT, GABA and ACh levels and aldicarb-induced paralysis assay

HPLC-MS/MS-based quantification of the four neurotransmitters DA, SRT, GABA and ACh revealed different quantities of all analytes in *C. elegans* (Fig. 5A–D). Untreated wildtype worms in young adult stage displayed 2.89 ng DA, 0.78 ng SRT, 529 ng GABA and 11.21 ng ACh each per mg of protein. Cu treatment failed to alter levels of all tested neurotransmitters compared to untreated controls in wildtype worms. In addition, in ceruloplasmin-deficient worms, Cu failed to induce any alterations in neurotransmitter levels, however, mutant strain ceruloplasmin displayed significantly reduced GABA levels compared to the wildtype. In contrast, atox-1-deficient worms had the similar basal levels of neurotransmitters in comparison to wildtype worms, but levels of DA, SRT, GABA and ACh were reduced upon treatment with 2 mM Cu for 24 h. The aldicarb-induced paralysis assay was used to examine alterations in the synaptic transmission rate at the neuromuscular junction in *C. elegans* [16,27]. Results revealed significant differences between wildtype and ceruloplasmin-deficient worms, as they displayed aldicarb resistance starting at 240 min aldicarb treatment compared to wildtype worms (Fig. 5E). Cu failed to alter the aldicarb-induced paralysis (Supplementary) and thus did not lead to changes in the synaptic transmission rate at the neuromuscular junction.

4. Discussion

Cu is an essential trace element, but is toxic when exceeding the homeostatic range, leading to oxidative stress [30]. Especially labile Cu, namely readily available Cu, is redox active and associated with neurodegenerative diseases, such as Wilson's disease (WD), Alzheimer's disease (AD) and Parkinson's disease (PD) [4,5]. However, the exact underlying mechanisms of Cu toxicity and neurotoxicity are poorly understood. It is therefore of paramount importance to shed light on molecular mechanisms of (labile) Cu-induced oxidative stress and neurotoxicity, which was addressed herein. We used *C. elegans* mutants with a disrupted Cu homeostasis and quantified, by a variety of highly specific and sensitive techniques, oxidative stress-related metabolites. Worm mutants lacking Cu chaperone atox-1 (ortholog in *C. elegans* is cuc-1) or the Cu binding protein ceruloplasmin (ortholog in *C. elegans* is F21D5.3) display elevated labile Cu levels, which was characterized in detail in our previous work [6].

MAP kinases induced by, among others, oxidative stress activate transcription factors like skn-1/NRF2 or daf-16/FOXO3, which then translocate into the nucleus to induce apoptosis, antioxidative defense or DNA repair [31]. Cu treatment led to a significant activation and translocalization of daf-16/FOXO3 in a concentration-dependent manner, corroborating earlier studies [32] and similar effects by other divalent metals like manganese (Mn) [33]. mRNA levels of *daf-16/FOXO3* remained unaffected after 24 h. However, as this is one of the first pathways affected by RONS, mRNA levels may have returned to normal. Urban et al. investigated gene expression levels of the antioxidant defense system over a time period of 10 days and display different time frames of up- and downregulation of genes related to oxidative stress [34]. Other studies reported Mn- and zinc-induced oxidative stress and neurotoxicity, but in that scenario *daf-16/FOXO3* mRNA levels were unaffected as well

[35]. Gene expression studies of representatives of the MAPK family revealed Cu-induced increase in *mpk-1/MAPK1* levels in wildtype worms, as well as altered basal levels in both deletion mutants of atox-1 and ceruloplasmin. He et al. corroborate these findings by displaying Cu-mediated cell death via p38 MAPK activation in vascular endothelial cells [36], while Wang et al. report the absence of Cu-induced apoptosis in *C. elegans* loss-of-function mutants of JNK and p38 MAP kinases [37], indicating the participation of MAPKs in the regulation of Cu-induced oxidative stress.

Cu overload increases the formation of RONS and leads to oxidative stress, which alters, among others, SOD or GPX activity, which then leads to oxidative stress [2,3]. It was shown that the GSH/GSSG ratio is reduced by Cu nanoparticles [36], supporting our data of reduced GSH and increased GSSG levels following Cu treatment. Notably, GSH levels were reduced by 23 % in wildtype worms, whereas by 38 % in ceruloplasmin-deficient worms, indicating a higher demand or consumption. A higher demand results in an increased synthesis [38], mediated by increased mRNA levels of *gcs*-1/GCLC in ceruloplasmin- and atox-1-deficient mutants. As stated above, Cu mediates p38 downstream activation of transcription factors like daf-16/FOXO3 or skn-1/NRF2, which activates gcs-1/GCLC expression [10]. GSH synthesis is ATP-dependent [39], potentially reducing ATP levels in ceruloplasmin-deficient worms, which are even further lowered by Cu treatment. Baldissera et al. also showed reduced hepatic ATP levels by Cu in *Cichlasoma amazonarum* [40]. In turn, levels of ADP and AMP, which are formed during ATP consumption [41], are increased by Cu supplementation in atox-1- and ceruloplasmin-deficient worms. In addition to GSH, Cu also alters GSSG levels in wildtype and atox-1 mutants, but significantly less in ceruloplasmin-deficient worms. This may indicate a higher rate of recycling or reducing GSSG back to GSH. This process is, among several others, NADPH-dependent, and is decreased in ceruloplasmin-deficient worms. Although this could be a possible explanation, it is noteworthy that energy-related nucleotides take part in other metabolic pathways as well. Thus, NAD^+ is formed in the GSH/GSSG cycling, which gets elevated by Cu treatment in ceruloplasmin-deficient worms. The Cu-sensing transcription factor Mac1 activates BNA expression and in turn quinolinic acid synthesis which results in *de novo* NAD^+ synthesis, which has been demonstrated in yeast [42,43]. Furthermore, Li et al. described a Cu-dependent S-Adenosylhomocysteine hydrolase inhibition, which results in a shift towards NAD^+ in the $NADH/NAD^+$ pool [44].

Recent studies have uncovered a rise in MDA levels subsequent to Cu treatment across various organisms [36,45,46], including *C. elegans* [2]. Our findings in wildtype worms demonstrated no alterations in either bound or unbound MDA levels, potentially attributed to our administration of (in wildtype worms) non-lethal Cu concentrations. Surprisingly, mutants deficient in atox-1 and ceruloplasmin exhibited comparable baseline levels of unbound MDA, yet notably heightened levels post-Cu treatment compared to wildtype worms. This suggests an increased hypersensitivity to Cu-induced oxidative stress or impaired antioxidative response under conditions of disrupted Cu homeostasis. CLs are vulnerable to oxidative damage due to their exclusive location within the inner mitochondrial membrane, where RONS are generated as byproduct of cellular respiration [47]. Oxidative stress can result in lipid oxidation and therefore in the formation of oxidized CL species [48]. Our findings indicate no observable formation of oxidized cardiolipins

following Cu incubation (data not shown). Blume et al. demonstrated a slight reduction in the total CL content following iron or manganese treatment, but no formation of oxidation products in *C. elegans* [49]. Furthermore, the distribution of individual CL species, known as the CL profile, remains unaffected by Cu exposure or the genetic makeup of the worms. It is noteworthy, however, that our analysis may not quantify all existing CL species, thus limiting our analysis to those above the detection threshold. Moreover, the data presented herein were solely in reference to untreated wildtype worms, as the establishment of improved standards and normalization procedures was essential for facilitating quantitative assessments. Nevertheless, the total sum of analyzed CL reveals a notable reduction in ceruloplasmin-deficient worms compared to the wildtype. Monteiro-Cardoso et al. stated that the total CL content drops significantly in the brain of an AD mouse model [13]. Several studies have also indicated that the dysregulation of CL content, as well as alterations of its structure and distribution, mediated neuronal dysfunction. These abnormalities are associated with the aging process and play a pivotal role in the pathogenesis of various neurodegenerative disorders, including AD and PD [12]. Aberrant levels of CLs have been linked to mitochondrial dysfunction, oxidative stress and impaired synaptic transmission, which are all hallmarks of AD and PD pathology. Understanding the mechanisms underlying cardiolipin-mediated neurodegeneration may offer novel therapeutic strategies aimed at preserving mitochondrial function and mitigating oxidative stress-related neuronal damage [12,13,50].

Cu and Cu nanoparticles have been shown to disrupt genomic integrity by causing oxidative DNA damage and DNA strand breaks [51, 52]. Thus, it is surprising that Cu failed to induce PARylation. This leads to a first assumption that possible DNA damages may already be repaired and that PAR was already degraded in our chronic exposure scenario of 24 h. However, 8oxodG, which is the most common DNA lesion [29], was significantly increased in ceruloplasmin-deficient worms following 24 h Cu incubation, refuting our first assumption. Like wildtype worms, ceruloplasmin mutants exhibited no alterations of PARylation levels, also this strain revealed Cu-induced DNA damage observed characterized by increased 8oxodG levels. PARylation is one of the largest consumers of NAD^+ [53]. Our data reveal normal levels of NAD^+ in wildtype worms and even further increased levels in ceruloplasmin mutants. At first glance, this indicates that NAD^+ deficiency can be ruled out as cause for normal PARylation levels. But it must be noted, that our data only reflect the total NAD^+ content instead of organell-specific selective NAD^+ levels. mRNA levels of *pme-1/PARP1* and *pme-2/PARP2* also remained unchanged in wildtype and ceruloplasmin-deficient worms. Taken together, these findings suggest that Cu inhibited PARylation, as previously hypothesized by Schwerdtle et al. [54]. Basal levels of PARylation were reduced in atox-1 mutants, possibly due to reduced Cu transport into the nucleus by the lack atox-1, but partially compensated by P-type ATPase ATP7B [55]. In addition, atox-1 interacts with PARPs in a detoured manner. Atox-1 induced the expression of MDC1, a crucial protein for double strand repair [56]. MDC1 interacts with aprataxin [57], which in turn works in concert with PARP's [58], which could explain lowered PARylation and *pme-2/PARP2* mRNA levels in atox-1-deficient mutants compared to wildtype worms. This needs to be further elucidated in *C. elegans*. Although 8oxodG levels were not altered in atox-1-deficient worms, Cu appeared to adversely affect the genomic stability of this

mutants, as Cu treatment increased both PARylation and *pme-2/PARP2* mRNA levels. The low basal PARylation raise further concerns, since inhibited PAR has been linked to cellular toxicity as well as neurological dysfunction [59]. Although herein excess Cu failed to cause genotoxicity in wildtype worms, our data underline the importance of a properly functioning Cu homeostasis for genomic integrity.

The loss of proper antioxidant capacity and energy production as well as impaired genomic integrity may cause neuronal death [4,60]. Cu is known to cause neurotoxicity and is associated with neurodegenerative diseases, such as WD [61,62]. Labile bound Cu is commonly mentioned in the context of Cu-induced neurotoxicity [5,63], but knowledge on underlying mechanisms is scarce. Ceruloplasmin-deficient worms revealed aldicarb-resistance, reflecting decreased synaptic transmission rate at the neuromuscular junction [16]. Dabbish et al. demonstrated a correlation between aldicarb-sensitivity and reduced GABA levels [64]. This is contrary to our findings, as ceruloplasmin mutants displayed, next to aldicarb-resistance, reduced GABA levels compared to wildtype worms, indicating that further unknown factors may be involved. One likely mechanism of reduced GABA levels in ceruloplasmin-deficient worms might be that excess Cu, as described by D'Ambrosi et al. [65], reduces GABA receptor activity, resulting in altered GABA levels. Atox-1 deletion mutant's basal levels of neurotransmitters remained unchanged compared to wildtype worms but were reduced due to 2 mM Cu treatment. Kelner et al. noted that atox-1 suppressed oxidative damage and promoted neuronal survival [66]. Furthermore, atox-1 is known to interact with α-synuclein and inhibit amyloid formation [67]. This is in agreement with our findings on Cu-mediated reduction in neurotransmitter levels due to the lack of atox-1, reflecting Cu-induced neurodegeneration upon loss of atox-1. Our data support that the dysregulation of Cu homeostasis leads to oxidative stress and subsequent detrimental effects on neurocellular pathways, underlining the importance of a properly working Cu homeostasis.

5. Conclusion

A comprehensive approach was adopted, employing specific and sensitive techniques to quantify metabolites related to oxidative stress with special focus on mitochondria, oxidative DNA damage, DNA damage response as well as neurodegeneration in the context of disrupted Cu homeostasis. Loss-of-function mutants of Cu chaperone atox-1 and ceruloplasmin displayed increased labile Cu levels despite lowered total Cu uptake [6] concomitant with increased oxidative stress, reduced mitochondrial ATP levels and CL content, as well as oxidative DNA damage and impaired neuronal health. Our data underline the essentiality of a proper Cu homeostasis and the importance of valuable markers, such as labile Cu, to diagnose Cu dyshomeostasis. Furthermore, our study highlights the importance of mitochondrial integrity for genomic and neuronal health. As a future perspective, understanding the intricate interplay of CL dysregulation and neurodegenerative processes holds significant promise for the development of therapeutic interventions preserving genomic and neuronal stability.

Supplementary Material

Refer to Web version on PubMed Central for supplementary material.

Acknowledgement

Wildtype worms (N2) and TJ356 were provided by CGC, which is funded by NIH Office Research Infrastructure Programs. Atox-1 and ceruloplasmin deletion mutants were provided by S. Mitani Lab (NBRP, Tokyo Women's Medical University, Japan).

Funding information

This work was supported by the DFG Research Unit TraceAge (FOR 2558, BO4103/4–2) and the DFG (INST 218/81–1 FUGG).

Data availability

Data will be made available on request.

References

[1]. Chen L, Min J, Wang F, Copper homeostasis and cuproptosis in health and disease, Signal Transduct. Targeted Ther. 7 (2022) 378, 10.1038/s41392-022-01229-y.

[2]. Zhang Y, Zhao C, Zhang H, Liu R, Wang S, Pu Y, Yin L, Integrating transcriptomics C elegans responds to copper induced aging, Ecotoxicol. Environ. Saf. 222 (2021) 112494, 10.1016/j.ecoenv.2021.112494. [PubMed: 34265532]

[3]. Song S, Zhang X, Wu H, Han Y, Zhang J, Ma E, Guo Y, Molecular basis for antioxidant enzymes in mediating copper detoxification in the nematode Caenorhabditis elegans, PLoS One 9 (2014) e107685, 10.1371/journal.pone.0107685. [PubMed: 25243607]

[4]. Squitti R, Faller P, Hureau C, Granzotto A, White AR, Kepp KP, Copper imbalance in alzheimer's disease and its link with the amyloid hypothesis: towards a combined clinical, chemical, and genetic etiology, J. Alzheimers. Dis. 83 (2021) 23–41, 10.3233/JAD-201556. [PubMed: 34219710]

[5]. Borchard S, Raschke S, Zak KM, Eberhagen C, Einer C, Weber E, Müller SM, Michalke B, Lichtmannegger J, Wieser A, Rieder T, Popowicz GM, Adamski J, Klingenspor M, Coles AH, Viana R, Vendelbo MH, Sandahl TD, Schwerdtle T, Plitz T, Zischka H, Bis-choline tetrathiomolybdate prevents copper-induced blood-brain barrier damage, Life Sci. Alliance 5 (2022), 10.26508/lsa.202101164.

[6]. Weishaupt A-K, Lamann K, Tallarek E, Pezacki AT, Matier CD, Schwerdtle T, Aschner M, Chang CJ, Stürzenbaum SR, Bornhorst J, Dysfunction in atox-1 and ceruloplasmin alters labile Cu levels and consequently Cu homeostasis in C. elegans, Front. Mol. Biosci 11 (2024) 1354627, 10.3389/fmolb.2024.1354627. [PubMed: 38389896]

[7]. Maares M, Haupt A, Schüßler C, Kulike-Koczula M, Hackler J, Keil C, Mohr I, Schomburg L, Süssmuth RD, Zischka H, Merle U, Haase H, A fluorometric assay to determine labile copper(II) ions in serum, Sci. Rep. 13 (2023) 12807, 10.1038/s41598-023-39841-9. [PubMed: 37550465]

[8]. Tassone G, Kola A, Valensin D, Pozzi C, Dynamic interplay between copper toxicity and mitochondrial dysfunction in alzheimer's disease, Life 11 (2021), 10.3390/life11050386.

[9]. Kim GH, Kim JE, Rhie SJ, Yoon S, The role of oxidative stress in neurodegenerative diseases, Exp. Neurobiol 24 (2015) 325–340, 10.5607/en.2015.24.4.325. [PubMed: 26713080]

[10]. Ferguson GD, Bridge WJ, The glutathione system and the related thiol network in Caenorhabditis elegans, Redox Biol. 24 (2019) 101171, 10.1016/j.redox.2019.101171. [PubMed: 30901603]

[11]. Grotto D, Santa Maria LD, Boeira S, Valentini J, Charão MF, Moro AM, Nascimento PC, Pomblum VJ, Garcia SC, Rapid quantification of malondialdehyde in plasma by high performance liquid chromatography-visible detection, J. Pharm. Biomed. Anal. 43 (2007) 619–624, 10.1016/j.jpba.2006.07.030. [PubMed: 16949242]

[12]. Falabella M, Vernon HJ, Hanna MG, Claypool SM, Pitceathly RDS, Cardiolipin, mitochondria, and neurological disease, Trends Endocrinol. Metabol. 32 (2021) 224–237, 10.1016/j.tem.2021.01.006.

[13]. Monteiro-Cardoso VF, Oliveira MM, Melo T, Domingues MRM, Moreira PI, Ferreiro E, Peixoto F, Videira RA, Cardiolipin profile changes are associated to the early synaptic mitochondrial dysfunction in Alzheimer's disease, J. Alzheimers. Dis. 43 (2015) 1375–1392, 10.3233/JAD-141002. [PubMed: 25182746]

[14]. Yurkova IL, Arnhold J, Fitzl G, Huster D, Fragmentation of mitochondrial cardiolipin by copper ions in the Atp7b−/− mouse model of Wilson's disease, Chem. Phys. Lipids 164 (2011) 393–400, 10.1016/j.chemphyslip.2011.05.006. [PubMed: 21645498]

[15]. Wandt VK, Winkelbeiner N, Bornhorst J, Witt B, Raschke S, Simon L, Ebert F, Kipp AP, Schwerdtle T, A matter of concern - trace element dyshomeostasis and genomic stability in neurons, Redox Biol. 41 (2021) 101877, 10.1016/j.redox.2021.101877. [PubMed: 33607499]

[16]. Weishaupt A-K, Kubens L, Ruecker L, Schwerdtle T, Aschner M, Bornhorst J, A reliable method based on liquid chromatography–tandem mass spectrometry for the simultaneous quantification of neurotransmitters in Caenorhabditis elegans, Molecules 28 (2023) 5373, 10.3390/molecules28145373. [PubMed: 37513246]

[17]. Patel D, Xu C, Nagarajan S, Liu Z, Hemphill WO, Shi R, Uversky VN, Caldwell GA, Caldwell KA, Witt SN, Alpha-synuclein inhibits Snx3-retromer-mediated retrograde recycling of iron transporters in S. cerevisiae and C. elegans models of Parkinson's disease, Hum. Mol. Genet. 27 (2018) 1514–1532, 10.1093/hmg/ddy059. [PubMed: 29452354]

[18]. Brenner S, The genetics of Caenorhabditis elegans, Genetics 77 (1974) 71–94, 10.1093/genetics/77.1.71. [PubMed: 4366476]

[19]. Porta-de-la-Riva M, Fontrodona L, Villanueva A, Ceron J, Basic Caenorhabditis ´ elegans methods: synchronization and observation, J. Vis. Exp e4019 (2012), 10.3791/4019.

[20]. Bornhorst J, Chakraborty S, Meyer S, Lohren H, Brinkhaus SG, Knight AL, Caldwell KA, Caldwell GA, Karst U, Schwerdtle T, Bowman A, Aschner M, The effects of pdr1, djr1.1 and pink1 loss in manganese-induced toxicity and the role of α-synuclein in C. elegans, Metallomics 6 (2014) 476–490, 10.1039/c3mt00325f. [PubMed: 24452053]

[21]. Livak KJ, Schmittgen TD, Analysis of relative gene expression data using real-time quantitative PCR and the 2(-Delta Delta C(T)) Method, Methods 25 (2001) 402–408, 10.1006/meth.2001.1262. [PubMed: 11846609]

[22]. Thiel A, Weishaupt A-K, Nicolai MM, Lossow K, Kipp AP, Schwerdtle T, Bornhorst J, Simultaneous quantitation of oxidized and reduced glutathione via LC-MS/MS to study the redox state and drug-mediated modulation in cells, worms and animal tissue, J. Chromatogr., B: Anal. Technol. Biomed. Life Sci 1225 (2023) 123742, 10.1016/j.jchromb.2023.123742.

[23]. Bornhorst J, Ebert F, Lohren H, Humpf H-U, Karst U, Schwerdtle T, Effects of manganese and arsenic species on the level of energy related nucleotides in human cells, Metallomics 4 (2012) 297–306, 10.1039/c2mt00164k. [PubMed: 22266671]

[24]. Grintzalis K, Zisimopoulos D, Grune T, Weber D, Georgiou CD, Method for the simultaneous determination of free/protein malondialdehyde and lipid/protein hydroperoxides, Free Radic. Biol. Med. 59 (2013) 27–35, 10.1016/j.freeradbiomed.2012.09.038. [PubMed: 23041350]

[25]. Nicolai MM, Weishaupt A-K, Baesler J, Brinkmann V, Wellenberg A, Winkelbeiner N, Gremme A, Aschner M, Fritz G, Schwerdtle T, Bornhorst J, Effects of manganese on genomic integrity in the multicellular model organism Caenorhabditis elegans, Int. J. Mol. Sci. 22 (2021), 10.3390/ijms222010905.

[26]. Neumann C, Baesler J, Steffen G, Nicolai MM, Zubel T, Aschner M, Bürkle A, Mangerich A, Schwerdtle T, Bornhorst J, The role of poly(ADP-ribose) polymerases in manganese exposed Caenorhabditis elegans, J. Trace Elem. Med. Biol. 57 (2020) 21–27, 10.1016/j.jtemb.2019.09.001. [PubMed: 31546209]

[27]. Mahoney TR, Luo S, Nonet ML, Analysis of synaptic transmission in Caenorhabditis elegans using an aldicarb-sensitivity assay, Nat. Protoc. 1 (2006) 1772–1777, 10.1038/nprot.2006.281. [PubMed: 17487159]

[28]. Ceballos MP, Parody JP, Quiroga AD, Casella ML, Francés DE, Larocca MC, Carnovale CE, Alvarez M.d.L., Carrillo MC, FoxO3a nuclear localization and its association with β-catenin and Smads in IFN-α-treated hepatocellular carcinoma cell lines, J. Interferon Cytokine Res. 34 (2014) 858–869, 10.1089/jir.2013.0124. [PubMed: 24950290]

[29]. Poetsch AR, The genomics of oxidative DNA damage, repair, and resulting mutagenesis, Comput. Struct. Biotechnol. J 18 (2020) 207–219, 10.1016/j.csbj.2019.12.013. [PubMed: 31993111]

[30]. Ge EJ, Bush AI, Casini A, Cobine PA, Cross JR, DeNicola GM, Dou QP, Franz KJ, Gohil VM, Gupta S, Kaler SG, Lutsenko S, Mittal V, Petris MJ, Polishchuk R, Ralle M, Schilsky ML, Tonks NK, Vahdat LT, van Aelst L, Xi D, Yuan P, Brady DC, Chang CJ, Connecting copper and cancer: from transition metal signalling to metalloplasia, Nat. Rev. Cancer 22 (2022) 102–113, 10.1038/s41568-021-00417-2. [PubMed: 34764459]

[31]. Peres TV, Arantes LP, Miah MR, Bornhorst J, Schwerdtle T, Bowman AB, Leal RB, Aschner M, Role of Caenorhabditis elegans AKT-1/2 and SGK-1 in manganese toxicity, Neurotox. Res 34 (2018) 584–596, 10.1007/s12640-018-9915-1. [PubMed: 29882004]

[32]. Hamann I, Petroll K, Grimm L, Hartwig A, Klotz L-O, Insulin-like modulation of Akt/FoxO signaling by copper ions is independent of insulin receptor, Arch. Biochem. Biophys. 558 (2014) 42–50, 10.1016/j.abb.2014.06.004. [PubMed: 24933099]

[33]. Gubert P, Puntel B, Lehmen T, Bornhorst J, Avila DS, Aschner M, Soares FAA, Reversible reprotoxic effects of manganese through DAF-16 transcription factor activation and vitellogenin downregulation in Caenorhabditis elegans, Life Sci. 151 (2016) 218–223, 10.1016/j.lfs.2016.03.016. [PubMed: 26972607]

[34]. Urban N, Tsitsipatis D, Hausig F, Kreuzer K, Erler K, Stein V, Ristow M, Steinbrenner H, Klotz L-O, Non-linear impact of glutathione depletion on C. elegans life span and stress resistance, Redox Biol. 11 (2017) 502–515, 10.1016/j.redox.2016.12.003. [PubMed: 28086197]

[35]. Baesler J, Michaelis V, Stiboller M, Haase H, Aschner M, Schwerdtle T, Sturzenbaum SR, Bornhorst J, Nutritive manganese and zinc overdosing in aging C. elegans result in a metallothionein-mediated alteration in metal homeostasis, Mol. Nutr. Food Res. 65 (2021) e2001176, 10.1002/mnfr.202001176. [PubMed: 33641237]

[36]. He H, Zou Z, Wang B, Xu G, Chen C, Qin X, Yu C, Zhang J, Copper oxide nanoparticles induce oxidative DNA damage and cell death via copper ion-mediated P38 MAPK activation in vascular endothelial cells, Int. J. Nanomed 15 (2020) 3291–3302, 10.2147/IJN.S241157.

[37]. Wang S, Wu L, Wang Y, Luo X, Lu Y, Copper-induced germline apoptosis in Caenorhabditis elegans: the independent roles of DNA damage response signaling and the dependent roles of MAPK cascades, Chem. Biol. Interact. 180 (2009) 151–157, 10.1016/j.cbi.2009.03.012. [PubMed: 19497412]

[38]. Franco R, Schoneveld OJ, Pappa A, Panayiotidis MI, The central role of glutathione in the pathophysiology of human diseases, Arch. Physiol. Biochem. 113 (2007) 234–258, 10.1080/13813450701661198. [PubMed: 18158646]

[39]. Cui C, Kong M, Wang Y, Zhou C, Ming H, Characterization of polyphosphate kinases for the synthesis of GSH with ATP regeneration from AMP, Enzym. Microb. Technol. 149 (2021) 109853, 10.1016/j.enzmictec.2021.109853.

[40]. Baldissera MD, Souza CF, Barroso DC, Pereira RS, Alessio KO, Bizzi C, Baldisserotto B, Val AL, Acute exposure to environmentally relevant concentrations of copper affects branchial and hepatic phosphoryl transfer network of Cichlasoma amazonarum: impacts on bioenergetics homeostasis, Comp. Biochem. Physiol. C Toxicol. Pharmacol 238 (2020) 108846, 10.1016/j.cbpc.2020.108846. [PubMed: 32777469]

[41]. Bonora M, Patergnani S, Rimessi A, de Marchi E, Suski JM, Bononi A, Giorgi C, Marchi S, Missiroli S, Poletti F, Wieckowski MR, Pinton P, ATP synthesis and storage, Purinergic Signal. 8 (2012) 343–357, 10.1007/s11302-012-9305-8. [PubMed: 22528680]

[42]. Croft T, Venkatakrishnan P, Lin S-J, NAD+ metabolism and regulation: lessons from yeast, Biomolecules 10 (2020), 10.3390/biom10020330.

[43]. James Theoga Raj C, Croft T, Venkatakrishnan P, Groth B, Dhugga G, Cater T, Lin S-J, The copper-sensing transcription factor Mac1, the histone deacetylase Hst1, and nicotinic acid

regulate de novo NAD+ biosynthesis in budding yeast, J. Biol. Chem. 294 (2019) 5562–5575, 10.1074/jbc.RA118.006987. [PubMed: 30760525]

[44]. Li M, Li Y, Chen J, Wei W, Pan X, Liu J, Liu Q, Leu W, Zhang L, Yang X, Lu J, Wang K, Copper ions inhibit S-adenosylhomocysteine hydrolase by causing dissociation of NAD+ cofactor, Biochemistry 46 (2007) 11451–11458, 10.1021/bi700395d. [PubMed: 17892301]

[45]. Anadozie SO, Aduma AU, Adewale OB, Alkaloid-rich extract of Buchholzia coriacea seed mitigate the effect of copper-induced toxicity in Drosophila melanogaster, Vegetos (2023), 10.1007/s42535-023-00760-9.

[46]. Rehman M, Maqbool Z, Peng D, Liu L, Morpho-physiological traits, antioxidant capacity and phytoextraction of copper by ramie (Boehmeria nivea L.) grown as fodder in copper-contaminated soil, Environ. Sci. Pollut. Res. Int. 26 (2019) 5851–5861, 10.1007/s11356-018-4015-6. [PubMed: 30613880]

[47]. Kowalczyk P, Sulejczak D, Kleczkowska P, Bukowska-Ósko I, Kucia M, Popiel M, Wietrak E, Kramkowski K, Wrzosek K, Kaczynska K, Mitochondrial ´ oxidative stress-A causative factor and therapeutic target in many diseases, Int. J. Mol. Sci. 22 (2021), 10.3390/ijms222413384.

[48]. Helmer PO, Nicolai MM, Schwantes V, Bornhorst J, Hayen H, Investigation of cardiolipin oxidation products as a new endpoint for oxidative stress in C. elegans by means of online two-dimensional liquid chromatography and high-resolution mass spectrometry, Free Radic. Biol. Med. 162 (2021) 216–224, 10.1016/j.freeradbiomed.2020.10.019. [PubMed: 33127566]

[49]. Blume B, Schwantes V, Witting M, Hayen H, Schmitt-Kopplin P, Helmer PO, Michalke B, Lipidomic and metallomic alteration of Caenorhabditis elegans after acute and chronic manganese, Iron, and Zinc exposure with a link to neurodegenerative disorders, J. Proteome Res. 22 (2023) 837–850, 10.1021/acs.jproteome.2c00578. [PubMed: 36594972]

[50]. Pope S, Land JM, Heales SJR, Oxidative stress and mitochondrial dysfunction in neurodegeneration; cardiolipin a critical target? Biochim. Biophys. Acta 1777 (2008) 794–799, 10.1016/j.bbabio.2008.03.011. [PubMed: 18420023]

[51]. Sadiq R, Khan QM, Mobeen A, Hashmat AJ, In vitro toxicological assessment of iron oxide, aluminium oxide and copper nanoparticles in prokaryotic and eukaryotic cell types, Drug Chem. Toxicol. 38 (2015) 152–161, 10.3109/01480545.2014.919584. [PubMed: 24896217]

[52]. Husain N, Mahmood R, Copper(II) generates ROS and RNS, impairs antioxidant system and damages membrane and DNA in human blood cells, Environ. Sci. Pollut. Res. Int 26 (2019) 20654–20668, 10.1007/s11356-019-05345-1. [PubMed: 31104239]

[53]. Bürkle A, Poly(ADP-ribose). The most elaborate metabolite of NAD+, FEBS J. 272 (2005) 4576–4589, 10.1111/j.1742-4658.2005.04864.x. [PubMed: 16156780]

[54]. Schwerdtle T, Hamann I, Jahnke G, Walter I, Richter C, Parsons JL, Dianov GL, Hartwig A, Impact of copper on the induction and repair of oxidative DNA damage, poly(ADP-ribosyl)ation and PARP-1 activity, Mol. Nutr. Food Res. 51 (2007) 201–210, 10.1002/mnfr.200600107. [PubMed: 17230584]

[55]. Karginova O, Weekley CM, Raoul A, Alsayed A, Wu T, Lee SS-Y, He C, Olopade OI, Inhibition of copper transport induces apoptosis in triple-negative breast cancer cells and suppresses tumor angiogenesis, Mol. Cancer Therapeut 18 (2019) 873–885, 10.1158/1535-7163.MCT-18-0667.

[56]. Jin J, Ma M, Shi S, Wang J, Xiao P, Yu H-F, Zhang C, Guo Q, Yu Z, Lou Z, Teng C-B, Copper enhances genotoxic drug resistance via ATOX1 activated DNA damage repair, Cancer Lett. 536 (2022) 215651, 10.1016/j.canlet.2022.215651. [PubMed: 35315340]

[57]. Becherel OJ, Jakob B, Cherry AL, Gueven N, Fusser M, Kijas AW, Peng C, Katyal S, McKinnon PJ, Chen J, Epe B, Smerdon SJ, Taucher-Scholz G, Lavin MF, CK2 phosphorylation-dependent interaction between aprataxin and MDC1 in the DNA damage response, Nucleic Acids Res. 38 (2010) 1489–1503, 10.1093/nar/gkp1149. [PubMed: 20008512]

[58]. Harris JL, Jakob B, Taucher-Scholz G, Dianov GL, Becherel OJ, Lavin MF, Aprataxin, poly-ADP ribose polymerase 1 (PARP-1) and apurinic endonuclease 1 (APE1) function together to protect the genome against oxidative damage, Hum. Mol. Genet. 18 (2009) 4102–4117, 10.1093/hmg/ddp359. [PubMed: 19643912]

[59]. Bornhorst J, Meyer S, Weber T, Böker C, Marschall T, Mangerich A, Beneke S, Bürkle A, Schwerdtle T, Molecular mechanisms of Mn induced neurotoxicity: RONS generation,

genotoxicity, and DNA-damage response, Mol. Nutr. Food Res. 57 (2013) 1255–1269, 10.1002/mnfr.201200758. [PubMed: 23495240]

[60]. Hegde ML, Hegde PM, Holthauzen LMF, Hazra TK, Rao KSJ, Mitra S, Specific Inhibition of NEIL-initiated repair of oxidized base damage in human genome by copper and iron: potential etiological linkage to neurodegenerative diseases, J. Biol. Chem. 285 (2010) 28812–28825, 10.1074/jbc.M110.126664. [PubMed: 20622253]

[61]. Minniti AN, Rebolledo DL, Grez PM, Fadic R, Aldunate R, Volitakis I, Cherny RA, Opazo C, Masters C, Bush AI, Inestrosa NC, Intracellular amyloid formation in muscle cells of Abeta-transgenic Caenorhabditis elegans: determinants and physiological role in copper detoxification, Mol. Neurodegener 4 (2009) 2, 10.1186/1750-1326-4-2. [PubMed: 19126228]

[62]. Metaxas A, Imbalances in copper or zinc concentrations trigger further trace metal dyshomeostasis in amyloid-beta producing Caenorhabditis elegans, Front. Neurosci. 15 (2021) 755475, 10.3389/fnins.2021.755475. [PubMed: 34707479]

[63]. Squitti R, Catalli C, Gigante L, Marianetti M, Rosari M, Mariani S, Bucossi S, Mastromoro G, Ventriglia M, Simonelli I, Tondolo V, Singh P, Kumar A, Pal A, Rongioletti M, Non-ceruloplasmin copper identifies a subtype of alzheimer's disease (CuAD): characterization of the cognitive profile and case of a CuAD patient carrying an RGS7 stop-loss variant, Int. J. Mol. Sci. 24 (2023), 10.3390/ijms24076377.

[64]. Dabbish NS, Raizen DM, GABAergic synaptic plasticity during a developmentally regulated sleep-like state in C. elegans, J. Neurosci. 31 (2011) 15932–15943, 10.1523/JNEUROSCI.0742-11.2011. [PubMed: 22049436]

[65]. D'Ambrosi N, Rossi L, Copper at synapse: release, binding and modulation of neurotransmission, Neurochem. Int. 90 (2015) 36–45, 10.1016/j.neuint.2015.07.006. [PubMed: 26187063]

[66]. Kelner GS, Lee M, Clark ME, Maciejewski D, McGrath D, Rabizadeh S, Lyons T, Bredesen D, Jenner P, Maki RA, The copper transport protein Atox1 promotes neuronal survival, J. Biol. Chem. 275 (2000) 580–584, 10.1074/jbc.275.1.580. [PubMed: 10617654]

[67]. Horvath I, Blockhuys S, Sulskis D, Holgersson S, Kumar R, Burmann BM, Wittung-Stafshede ˇP, Interaction between copper chaperone Atox1 and Parkinson's disease protein α-synuclein includes metal-binding sites and occurs in living cells, ACS Chem. Neurosci. 10 (2019) 4659–4668, 10.1021/acschemneuro.9b00476. [PubMed: 31600047]

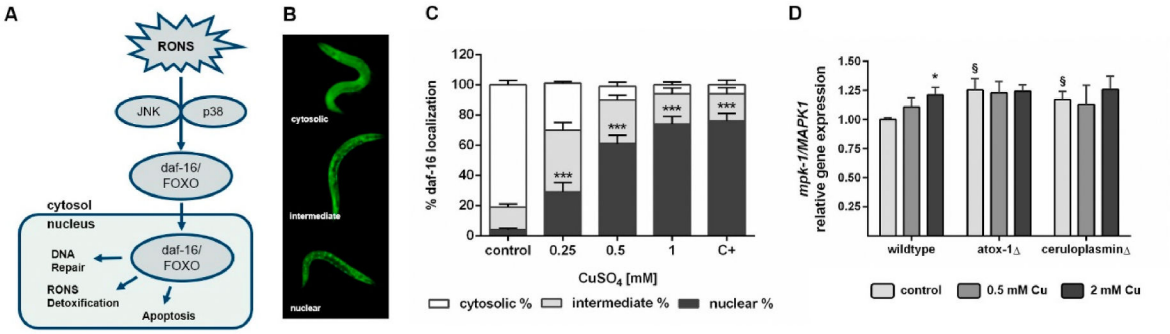

Fig. 1.

(A) Schematic daf-16 translocation from cytosol into the nucleus under oxidative stress conditions. (B) Exemplary fluorescence images of worms displaying cytosolic, intermediate or nuclear localized daf-16 in mutant worm daf-16::GFP. (C) daf-16 localization [%] of worms treated 24 h with $CuSO_4$ or PQ as positive control (C+). Presented are mean values of n = 3 (N = 25) independent experiments +SEM. (D) Relative mRNA levels of *mpk-1/MAPK1* following 24 h Cu incubation. Data presented are mean values of n = 4 independent experiments +SEM.

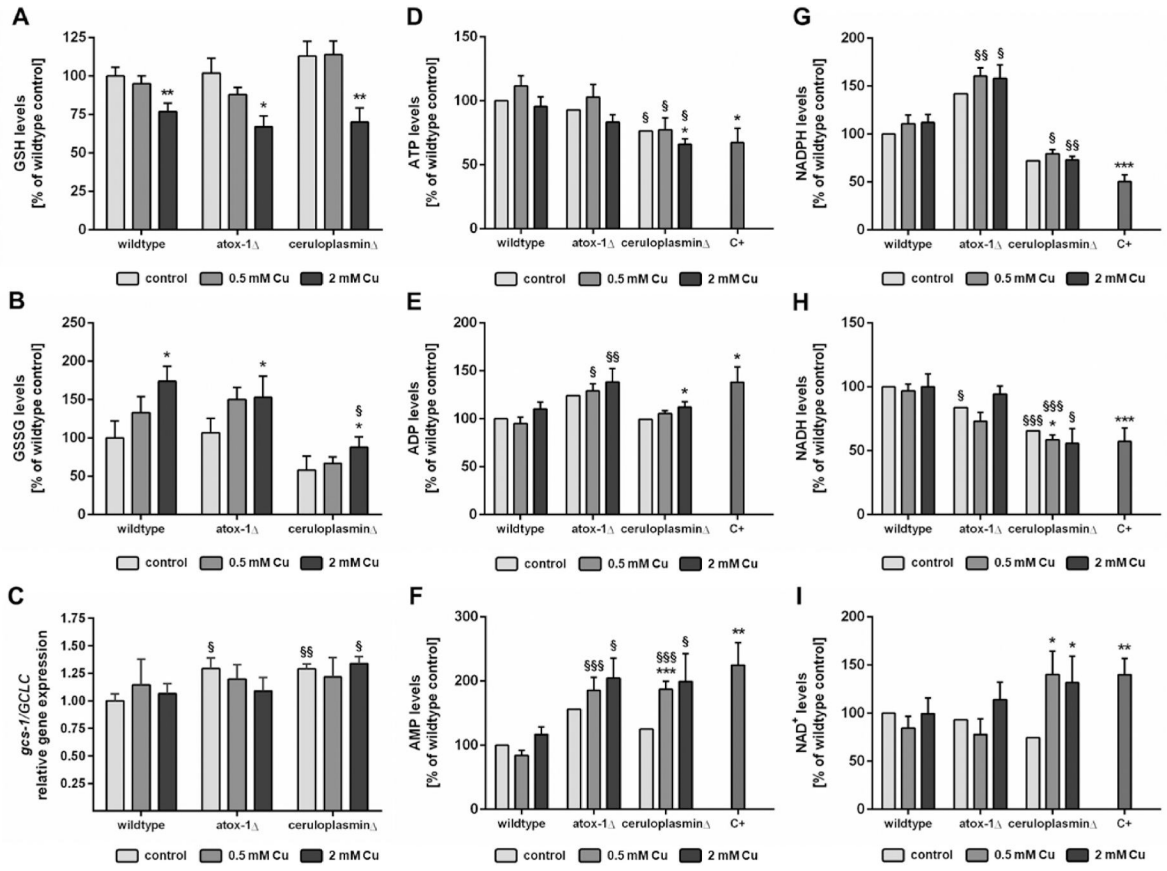

Fig. 2.

(A) GSH and (B) GSSG levels normalized to wildtype control [%]. (C) Relative mRNA levels of *gcs*-1/GCLC. Levels of (D) ATP, (E) ADP, (F) AMP, (G) NADPH, (H) NADH and (I) NAD^+ compared to wildtype control [%]. PQ was used as positive control (C+) in wildtype worms. Data presented are mean values of $n \geq 4$ independent experiments +SEM.

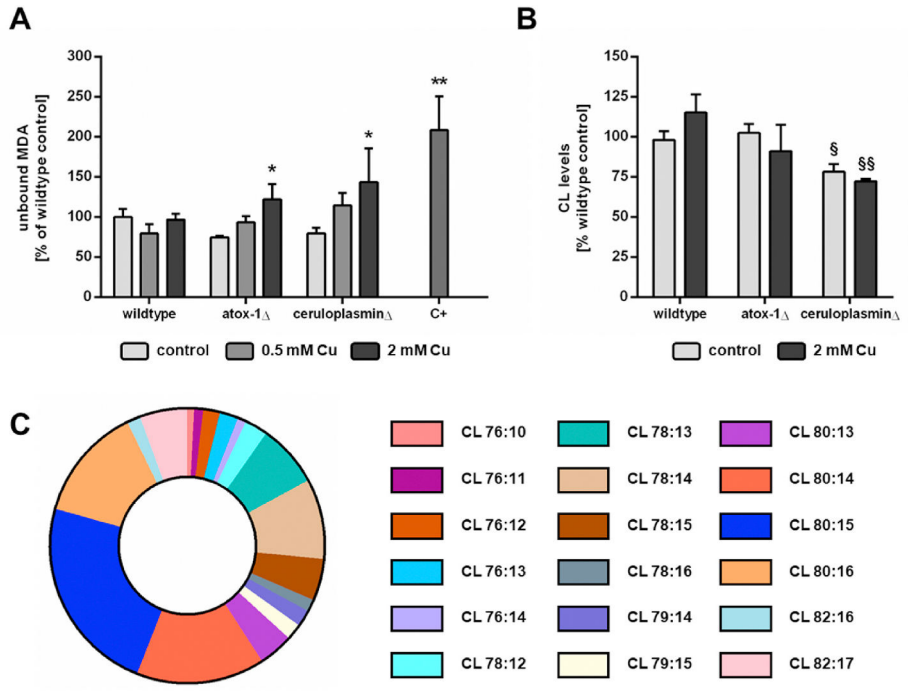

Fig. 3.

(A) MDA levels (unbound) normalized to wildtype control [%]. *t*-BOOH was used as positive control (C+) in wildtype worms. Data presented are mean values of n = 4 independent experiments +SEM. (B) Total CL levels normalized to protein content and to wildtype control [%]. Data presented are mean values of n ≥ 3 independent experiments +SEM. (C) Representative distribution of CL species in terms of chain length and degree of saturation for untreated wildtype worms.

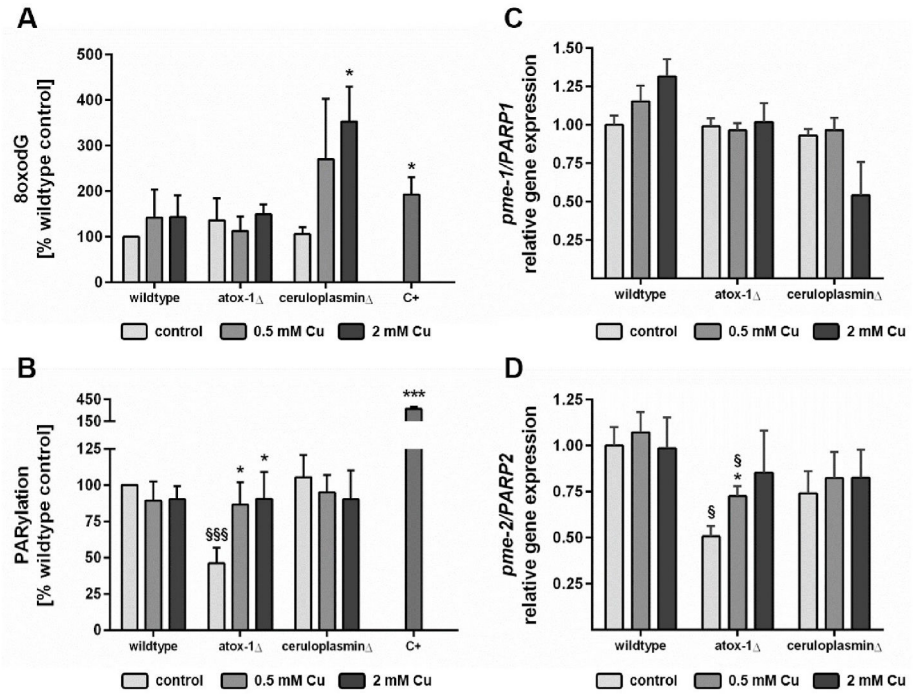

Fig. 4.

Relative (A) 8oxodG and (B) PARylation levels normalized to wildtype control [%]. As positive control (C+) *t*-BOOH was used in wildtype worms. Relative mRNA levels of (C) *pme-1/PARP1* and (D) *pme-2/PARP2* following 24 h Cu incubation. Data presented are mean values of n = 4 independent experiments +SEM.

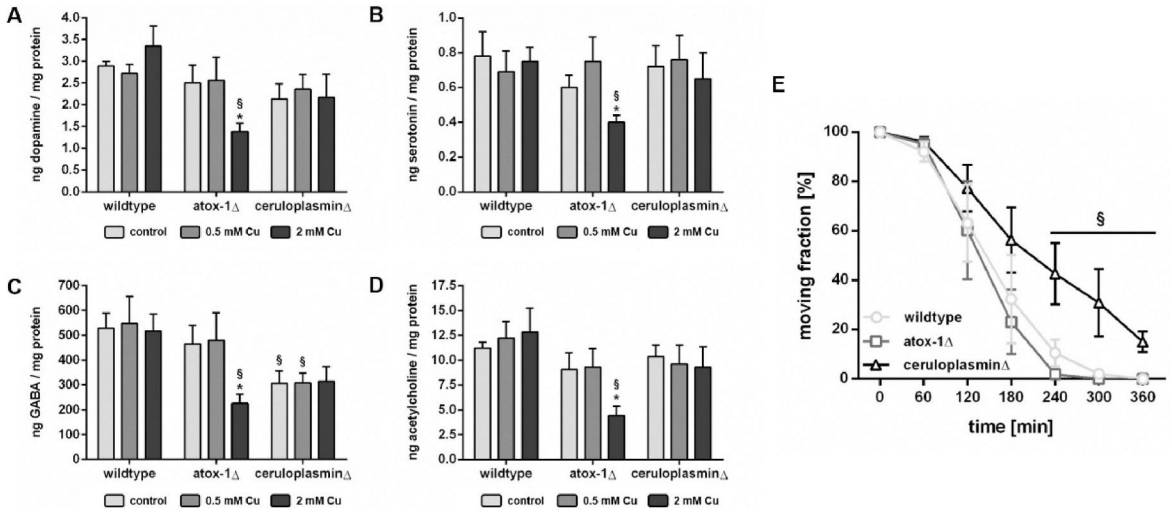

Fig. 5.

Neurotransmitter levels in ng per mg protein in *C. elegans* quantified via HPLC-MS/MS. Assessed were levels of (A) DA, (B) SRT, (C) acid GABA and (D) ACh. Aldicarb-induced paralysis assay in (E) untreated wildtype (light grey), atox-1Δ (dark grey) and ceruloplasminΔ (black) worms. Plotted are the fraction of moving worms [%] against the assay procedure time [min]. Data presented are mean values of $n \geq 4$ independent experiments ± SEM.